Homeodomain-interacting protein kinase (Hipk) is required for nervous system and muscle structure and function

Simon Wang[2,3], Donald A.R. Sinclair[1,3], Hae-Yoon Kim[1,3], Stephen D. Kinsey[1,3], Byoungjoo Yoo[1,3], Kenneth Kin-Lam Wong[1,3], Charles Krieger[2,3], Nicholas Harden[1,3], Esther M. Verheyen[1,3, *]

[1]Department of Molecular Biology and Biochemistry

[2]Department of Biomedical Physiology and Kinesiology

[3]Centre for Cell Biology, Development and Disease

Simon Fraser University, Burnaby, V5A 1S6, Canada

* Corresponding author: everheye@sfu.ca

1

1 **Abstract:**

2   Homeodomain-interacting protein kinases (Hipk) have been previously associated with cell

3   proliferation and cancer, however, their effects in the nervous system are less well understood.

4   We have used *Drosophila melanogaster* to evaluate the effects of altered Hipk expression on the

5   nervous system and muscle. Using genetic manipulation of Hipk expression we demonstrate that

6   knockdown and over-expression of Hipk produces early adult lethality, partially due to the

7   effects on the nervous system and muscle involvement. We find that optimal levels of Hipk are

8   critical for the function of dopaminergic neurons and glial cells in the nervous system, as well as

9   muscle. Furthermore, manipulation of Hipk affects the structure of the larval neuromuscular

10   junction (NMJ) and increases motor neuron axonal branching. Hipk regulates the

11   phosphorylation of the synapse-associated cytoskeletal protein Hts (adducin) and modulates the

12   expression of two important protein kinases, Calcium-calmodulin protein kinase II (CaMKII)

13   and Partitioning-defective 1 (PAR-1), all of which may alter neuromuscular function and

14   influence lethality. Hipk also modifies the distribution of an important nuclear protein, TBPH,

15   the fly orthologue of TAR DNA-binding protein 43 (TDP-43), which may have relevance for

16   understanding motor neuron diseases.

17

18 **Introduction:**

19   Homeodomain-interacting protein kinase (Hipk) family members constitute a group of serine

20   threonine kinases that phosphorylate many homeodomain transcription factors and influence cell

21   proliferation and tissue growth (Blaquiere and Verheyen, 2017; Kim et al., 1998). In *Drosophila*,

22   the single Hipk family member is essential for embryonic and larval survival and when over-

23   expressed, acts as a potent growth regulator that can stimulate tumorigenesis and metastatic cell

24   behavior through its actions on many signaling pathways including Wnt/Wingless, Hippo, Notch

25   and JNK (Blaquiere et al., 2018; Chen and Verheyen, 2012; Huang et al., 2011; Kim et al., 1998;

26   Lee et al., 2009a; Poon et al., 2012; Swarup and Verheyen, 2011). In *C. elegans*, the single Hipk

27   ortholog, HPK-1, does not appear to be essential during development, but an *HPK-1* mutant

28   significantly shortens adult lifespan (Berber et al., 2016). Vertebrates possess four Hipk

29   orthologs that have some conserved and additional divergent functions (reviewed in Blaquiere

30   and Verheyen, 2017). Numerous studies suggest that Hipk family members may also influence

31 signaling pathways related to nervous system development and function. Flies with reduced

32 dHipk possess small eyes with neuronal abnormalities (Blaquiere et al., 2014; Lee et al., 2009b).

33 *Hipk1 Hipk2* double knockout mice are embryonic lethal and have underdeveloped retinas and

34 defects in neural tube closure (Aikawa et al., 2006; Inoue et al., 2010; Isono et al., 2006). Mouse

35 Hipk2 regulates the survival of sensory and sympathetic neurons, and midbrain dopamine

36 neurons (Doxakis et al., 2004; Wiggins et al., 2004; Zhang et al., 2007a). In the embryonic

37 midbrain, loss of mouse Hipk2 leads to a decrease in the number of neurons, resulting in

38 Parkinson's disease-like psychomotor abnormalities (Zhang et al., 2007a).

39 The relative level of expression of the *hipk* gene in the nervous system of larvae and adults is

40 robust as described in Flybase (Thurmond et al., 2019). For these reasons, we explored the

41 potential involvement of Hipk in the structure and function of the *Drosophila* nervous system.

42 We show that down-regulation or over-expression of Hipk pan-neurally, as well as in

43 dopaminergic neurons, glial cells and muscle cells is lethal. However, Hipk mis-expression in

44 motor neurons, cholinergic or glutamatergic neurons has no obvious effects on viability. To

45 investigate the potential causes of lethality from altered expression of Hipk, we focus on

46 larvalneuromuscular junctions (NMJ) and muscle and find that Hipk regulates motor axon

47 outgrowth and several synaptic proteins including Hts/adducin, Calcium/calmodulin-dependent

48 protein kinase II (CaMKII) and PAR-1 (Partitioning-defective 1; a fly orthologue of microtubule

49 affinity-regulating kinase). These studies demonstrate that Hipk regulates NMJ and muscle

50 organization.

51

52 **Results:**

53 **Modulation of Hipk in adults leads to premature death**

54 Since it has been shown that a *C. elegans HPK-1* mutant shortens adult lifespan (Berber et al.,

55 2016), we decided to investigate the role of Hipk in adult *Drosophila* using the Gal4-UAS

56 expression system in combination with a temperature sensitive *Gal80^{ts}* repressor to over-express

57 and to knock-down Hipk after eclosion. We grew flies at 18°C until adulthood, and then shifted

58 them to 29°C to inactivate the *Gal80^{ts}* repressor and to optimize Gal4 transcriptional activation of

59 the UAS constructs. To rule out sex differences we used males in all adult survival analyses. For

60   most studies, we utilized the 17090R-1 RNAi line from the National Institute of Genetics (NIG)

61   to knock down *hipk* gene expression and will refer to this as *UAS-hipk-RNAi*, unless otherwise

62   noted. We first assessed viability of adult males following *hipk* knockdown. The vast majority of

63   *UAS-hipk-RNAi/Gal80^{ts}; Tub-Gal4/+* males died within 2-4 days after they were shifted from

64   18°C to 29°C (Fig. 1, red curves). With ubiquitous over-expression of Hipk using the HA-tagged

65   *UAS-hipk^{3M}* transgene, (hereafter referred to as *UAS-hipk*), all *Gal80^{ts}/+; UAS-hipk/Tub-Gal4*

66   males died within approximately 7-10 days after they were shifted from 18°C to 29°C (Fig. 1,

67   green curves). Typically, for both over-expression and knockdown experiments, there was a very

68   small number of experimental flies that escaped early death. In both cases, prior to death, the

69   activity of experimental males slowed progressively until they appeared immobile. In contrast,

70   identically-treated internal control (Fig. 1, blue curves) and Oregon-R control (Fig. 1, grey

71   curves) males survived considerably longer. These data indicate that both RNAi-induced

72   knockdown and over-expression of Hipk dramatically affects survival and movement of males,

73   suggesting the possibility that the flies may have impaired neural, and/or muscle function.

74   **Modulation of Hipk during development affects specific cell types in the nervous system, as**

75   **well as muscle cells**

76   Based on these observations, we examined developmental effects of Hipk knockdown and over-

77   expression at 29°C using several nervous system *Gal4* drivers and *Mef2-Gal4*, a muscle-specific

78   driver (Tables 1, 2). Pan-neural knockdown of Hipk with *Appl-Gal4* resulted in complete

79   lethality with a polyphasic lethal phase. To dissect this effect further we knocked down gene

80   expression in subsets of neurons, namely dopaminergic, cholinergic, glutamatergic and motor

81   neurons. As shown in Table 1, knockdown in dopaminergic neurons using *ple-Gal4* and *TH-*

82   *Gal4* caused larval/pupal lethality, while knockdown in the other neurons did not affect viability.

83   Knockdown using the pan-neural driver *elav-Gal4* resulted in rough eyes in adults (Fig. 2B). In

84   addition, it is notable that Hipk knockdown in glial cells was also lethal, with a larval lethal

85   phase. Finally, Hipk knockdown in muscle cells caused lethality at the pupal stage.

86   To complement the knockdown experiments, we used the same *Gal4* driver strains to assess the

87   effects of over-expression of Hipk during development using *UAS-hipk* (Table 2). We observed

88   lethality at larval and pupal stages upon pan-neural expression using *Appl-Gal4*. In contrast, use

89   of *elav-Gal4* resulted in rough eyes (Fig. 2D). Moreover, Hipk over-expression using *UAS-hipk*

90   in combination with *longGMR-Gal4* generated flies with an abnormal glassy eye/reduced

91   pigmentation phenotype (Fig. 2F). These studies highlight that both gain or loss of Hipk in

92   neurons can affect eye formation and we have previously shown that Hipk is required during

93   larval development for eye specification (Blaquiere et al., 2014). Furthermore, as was the case

94   for Hipk knockdown, over-expression in dopaminergic neurons (larval lethal phase, LP), glial

95   cells (larval LP) and muscle cells (larval/pupal LP) was lethal, but over-expression in

96   cholinergic, glutamatergic or motor neurons was not.

97   Since Hipk knockdown in muscles and dopaminergic neurons during development was lethal, we

98   carried out a second set of adult survival experiments to see whether such knockdown affected

99   adult lifespan. For comparison, we included tests of ubiquitous over-expression of Hipk in

100   adults. The data show that Hipk knockdown in muscle cells does indeed cause early adult death;

101   nearly all of the *UAS-hipk-RNAi/+*; *Mef2-Gal4/Gal80^{ts}* males died within approximately 11-15

102   days at 29°C, in comparison to the control males (Fig. S1, purple versus black curves). However,

103   Hipk knockdown in dopaminergic neurons using *TH-Gal4* males had lifespans similar to those of

104   control males (Fig. S1, yellow versus black curves). Data for ubiquitous knockdown (Fig. S1, red

105   curve) and over-expression (Fig. S1, green curve) in adults were very similar to the results

106   described above. In summary, it appears that there is an essential requirement for Hipk in adult

107   muscles, but not in adult dopaminergic neurons. In a pilot study, we found that Hipk over-

108   expression in muscles of adult males did not affect survival (data not shown).

109   We extended the developmental analysis in a second set of experiments using a different RNAi

110   transgene *UAS-hipk*-RNAi (V2) and a second Hipk-expressing transgene *UAS-hipk* (attP40) and

111   a subset of nervous system and muscle *Gal4* drivers. The data indicate that, similar to the results

112   for the NIG *hipk*-RNAi transgene, the V2 UAS-*hipk*-RNAi transgene was lethal when expressed

113   in muscles and semi-lethal when expressed throughout the nervous system (Supplementary Table

114   1). However, in contrast to the previous knockdown data, V2 *UAS-hipk-RNAi*-induced

115   knockdown in dopaminergic neurons as well as in glial cells, had no effect. In addition, in

116   agreement with the previous over-expression data, the attP40 *UAS-hipk* transgene is lethal/semi-

117   lethal when expressed throughout the nervous system and semi-lethal when expressed in

118   dopaminergic neurons (Supplementary Table 2). However, in contrast to the previous

119   overexpression data, expression of the attP40 *UAS-hipk* transgene in muscles and glial cells had

5

120   no effect. Moreover, neither V2 *UAS-hipk* RNAi nor attP40 *UAS-hipk* generated a rough eye

121   phenotype when driven with *elav-Gal4* or *longGMR-Gal4* (data not shown). We believe that the

122   aforementioned differences in the data are due to variable potency of the V2 *UAS-hipk*-RNAi

123   and attP40 *UAS-hipk* transgenes. Collectively, our data suggest that Hipk regulates elements of

124   the fly nervous system and that Hipk causes lethality when mis-expressed in a subset of neurons

125   and glial cells. In addition, the lethal effects of perturbation of Hipk in muscle indicate essential

126   roles in the development and/or function of the tissue.

127   **Hipk is present in the muscle cytoplasm and nuclei during larval NMJ development, and**

128   **regulates NMJ size**

129   As modulation of Hipk levels with *Mef2-Gal4* caused pupal lethality, we examined the

130   distribution of Hipk at the neuromuscular junction (NMJ) of 3rd instar larvae. In wild-type, Hipk

131   immunoreactivity was observed as punctate labeling throughout the muscle cytoplasm and

132   within the DAPI-negative regions of muscle nuclei, with no obvious accumulations at the NMJ

133   (Fig. 3A-A'", C-C''). Muscle-specific Hipk over-expression led to increased Hipk extra-synaptic

134   puncta (Fig 3B-B'''). Most strikingly, however, muscle nuclei displayed considerable Hipk

135   immunoreactivity in the form of large, round bodies that consisted of strong Hipk labeling at the

136   surface of these structures with an internal core area containing less Hipk labeling (Fig. 3B'-B'",

137   D-D''). These structures were present in the DAPI-negative regions of the nucleus but did not

138   localize within the nucleolus.

139   Due to the presence of Hipk during larval NMJ development, we next tested for Hipk-mediated

140   effects on NMJ size and found that the NMJs of *Mef2*-driven Hipk over-expressors were

141   significantly larger than the NMJs of the wild-type controls (Fig 3A, B, E). Expression of

142   transgenic *hipk-RNAi* in the muscle caused severe muscle morphological defects (Fig. S2B) and

143   was not analyzed further in this study. As Hipk did not specifically localize to either the pre- or

144   post-synapse of the NMJ at endogenous or over-expressed levels, Hipk regulation of NMJ size

145   likely arises from indirect modulation of synaptic proteins.

146   **Hipk regulates multiple post-synaptic proteins, including the cytoskeletal protein, Hts**

147   To elucidate Hipk's role in regulating NMJ size in the muscle, we assessed the distribution of

148   multiple post-synaptic proteins in Hipk over-expressing larvae. No effects on the synaptic levels

6

149   of GluRIIA were observed between muscle-specific Hipk over-expression and the wild-type

150   control (Fig. S3A). However, over-expression of Hipk resulted in significantly lower α-Spectrin

151   levels (Fig. S3B) but higher Fasciclin 2 levels (Fig. S3C) at the NMJ. As the mode of regulation

152   differed between the post-synaptic proteins evaluated, the observed alterations associated with

153   Hipk over-expression appear to be specific, and not due to artificial or non-specific causes.

154   Another post-synaptic protein that has been shown to regulate NMJ growth is the actin-spectrin

155   associated protein, adducin/Hts (Pielage et al., 2011; Wang et al., 2011). In wild-type control

156   NMJs, Hts predominately localized to the postsynaptic membrane (Fig. 4A-A''). Hts was also

157   present extra-synaptically throughout the muscle membrane as punctate structures organized in a

158   lattice-like pattern (Fig. 4E), a distribution that is observed with spectrin networks in other

159   systems (Han et al., 2017; Xu et al., 2013). Muscle-specific over-expression of Hipk caused no

160   observable effects on Hts localization at the NMJ (Fig. 4B-B''). However, Hts distribution

161   throughout the extra-synaptic muscle membrane was either undetectable or disrupted (Fig. 4F).

162   In addition, aberrant accumulations of Hts often formed (Fig. 4G). These results indicate that

163   Hipk negatively regulates Hts extra-synaptic distribution at the muscle membrane.

164   In many cell types, phosphorylation of adducin/Hts by protein kinase C (PKC) or cAMP-

165   dependent protein kinase (PKA) can inhibit the interactions of adducin/Hts with the spectrin-

166   actin cytoskeleton, and cause adducin/Hts to redistribute from the plasma membrane to the

167   cytoplasm (Matsuoka et al., 1998). To determine if Hipk affects Hts distribution at the muscle

168   membrane through phosphorylation, we used an antibody that detects phosphorylation of the

169   mammalian adducins at the PKC/PKA target site in the myristoylated alanine-rich C-kinase

170   (MARCKS) domain. The site is conserved in *Drosophila* Hts, and the antibody has been

171   previously used on larval muscles to detect Hts phosphorylation (Wang et al., 2014). In the wild-

172   type control, Hts phosphorylation was observed at the NMJ, and was also present as puncta that

173   formed the lattice-like network in the muscle described above (Fig. 4C-C'', H). Muscle-specific

174   over-expression of Hipk suppressed Hts phosphorylation, as lower levels of p-adducin

175   immunoreactivity were observed at the NMJ (Fig. 4D-D''), and the lattice-like network in the

176   muscle was missing (Fig. 4I). In addition, aberrant accumulations in the muscle cytoplasm were

177   also observed (Fig. 4J). These results indicate that Hipk influences the phosphorylation of Hts,

178   either directly or indirectly.

7

Hipk suppresses CaMKII and PAR-1 expression, thus modulating Dlg phosphorylation

179

180   We have previously shown that Hts regulates the post-synaptic localization of the important

181   scaffolding molecule, Discs large (Dlg), by elevating the levels of the kinases, CaMKII and

182   PAR-1, in the muscle (Wang et al., 2011). CaMKII and PAR-1 phosphorylate Dlg at the PDZ1

183   and GUK domains, respectively, which disrupts Dlg postsynaptic targeting (Koh et al., 1999;

184   Zhang et al., 2007b) and influences synaptic stability (Krieger et al., 2016). To assess if Hipk

185   modulates this function of Hts, CaMKII and PAR-1 immunoreactivity were observed in the

186   muscles of control and Hipk over-expressing larvae. CaMKII and PAR-1 typically localize to the

187   NMJ, but are also present throughout the muscle (Fig. 5A, C), as shown previously (Koh et al.,

188   1999; Zhang et al., 2007b). When Hipk was over-expressed in the muscle, immunoreactivity

189   against CaMKII and PAR-1 was reduced (Fig. 5B, D). PAR-1 immunoreactivity at the muscle

190   membrane was missing in comparison to the wild-type control (compare corresponding cross-

191   sections for Fig. 5D, C). CaMKII immunoreactivity at the muscle membrane was also reduced,

192   revealing the underlying striated pattern of the sarcomeres (compare cross-sections for Fig. 5B,

193   A). To determine if the observed decreases in CaMKII and PAR-1 immunoreactivity were due to

194   changes at the transcript level, FISH was performed with the use of labeled antisense probes that

195   bind to *camkII* and *par-1* mRNA. Endogenous *camkII* and *par-1* transcripts appeared as puncta

196   throughout the muscle cytoplasm, with prominent accumulations found within muscle nuclei

197   (Fig. 5E-E'', G-G'') (Wang et al., 2014). However, muscle-specific Hipk over-expression caused

198   overall reductions in the levels of both transcripts (Fig. 5F-F'', H-H''; quantifications in Fig

199   S4A, B). These results indicate that Hipk suppresses the expression of CaMKII and PAR-1 at the

200   transcript level, thereby modifying the levels and distribution of these kinases in the muscle.

201   We next assessed whether Hipk also regulates Dlg by evaluating potential Hipk-mediated effects

202   on Dlg phosphorylation. To accomplish this, we made use of an antibody that specifically detects

203   Dlg phosphorylation at the PAR-1 target site (Zhang et al., 2007b). Unfortunately, no antibody

204   against phosphorylation at the CaMKII target site was available, thus we were unable to test this

205   directly. In the wild-type control, p-Dlg^{S797} immunoreactivity was observed at the NMJ and as

206   puncta throughout the muscle cytoplasm (Fig. 5I), as previously reported (Wang et al., 2011;

207   Zhang et al., 2007b). However, when Hipk was over-expressed in the muscle, extra-synaptic p-

208   Dlg puncta levels were significantly decreased (Fig. 5J; quantification in Fig. S4C). Collectively,

8

209   the data indicate that Hipk can modulate the phosphorylation of Dlg by PAR-1, and likely

210   CaMKII as well, through negatively regulating the expression of these kinases.

Hipk modulates the localization of nuclear proteins

212   The nuclear Hipk proteins have been previously associated with nuclear structures known as

213   'Hipk domains' (Moller et al., 2003), PML bodies, or paraspeckles (Rinaldo et al., 2008). To

214   further investigate the relationship between the striking nuclear Hipk structures observed on

215   Hipk over-expression and that of other nuclear factors, we performed immunocytochemistry with

216   antibodies to two nuclear proteins demonstrated to have extensive roles in the nervous system.

217   For instance, TAR DNA binding protein 43 (TDP-43) is a DNA- and RNA-binding protein

218   predominantly localized to the nucleus that has roles in transcriptional regulation, as well as

219   RNA processing and stability (Buratti and Baralle, 2001; Casci and Pandey, 2015). This protein

220   is present in *Drosophila*, where it has been well characterized and is called TBPH (Casci and

221   Pandey, 2015). Additionally, the protein fused in sarcoma (FUS/TLS) ,which in *Drosophila* is

222   represented by Cabeza (Caz, or dFUS), is a nuclear-associated transcriptional activator which has

223   also been well characterized (Lanson et al., 2011). Mutations in TDP-43 and FUS have been

224   identified in patients with the familial form of the neurodegenerative disorder amyotrophic

225   lateral sclerosis (ALS), which is characterized by progressive loss of motoneurons and muscle

226   atrophy.

227   In the wild-type control, Caz localized predominately to muscle nuclei (Fig. 6A). Muscle-

228   specific Hipk over-expression did not alter Caz distribution or levels (Fig. 6B). TBPH

229   immunoreactivity in the wild-type showed a largely nuclear distribution, with some labeling of

230   the muscle cytoplasm (Fig. 6C). In contrast, with Hipk over-expression, TBPH immunoreactivity

231   was strikingly reduced in the nucleus, with increased TBPH labelling around the nuclear

232   membrane (Fig. 6D). The presence of cytoplasmic TDP-43/TBPH is seen in a variety of

233   neurological disorders including ALS, as well as fly models of ALS, and is believed to be due to

234   the inability of TDP-43 to re-enter the nucleus (Casci and Pandey, 2015; Chou et al., 2018).

235   A deleterious interaction between Hipk overexpression and TBPH overexpression was seen

236   when Hipk (using attP40 *UAS-hipk*, which itself does not cause an eye phenotype when driven

237   with *longGMR-Gal4*) was co-expressed with *UAS-TBPH* in *Drosophila* eyes, using *longGMR-*

9

238   *Gal4*, leading to a rough/necrotic eye phenotype (Fig 6I). On the other hand, analogous co-

239   expression of *UAS-caz* had no striking effect (Fig 6G).

240   **Discussion:**

241   Previous work has shown that elevated expression of Hipk leads to tumorigenesis and metastatic

242   cell behavior, likely by stimulating various signaling pathways such as Wnt/Wingless, Hippo,

243   Notch and JNK (Blaquiere et al., 2018; Chen and Verheyen, 2012; Huang et al., 2011; Lee et al.,

244   2009a, 2009c; Poon et al., 2012). However, relatively little is known regarding the action of Hipk

245   in the nervous system and muscle. We find that ubiquitous over-expression and knockdown of

246   Hipk have dramatic effects on adult survival, leading to progressive immobility and death and

247   these effects are most likely due to perturbations in the nervous system and muscle. Evidence for

248   nervous system involvement during development is supported by the observation of rough eye

249   phenotypes associated with pan-neural and/or eye-specific Hipk knockdown and over-

250   expression, as well as by the fact that such mis-expression in dopaminergic neurons and glial

251   cells is lethal. Taken together, these results show that both reduced and excessive levels of Hipk

252   have profound effects on nervous system function in flies. Our adult-specific data are consistent

253   with observations that *hipk2* knockout mice exhibit increased perinatal lethality and that a

254   mutation in the *C. elegans* ortholog, *hpk-1*, shortens lifespan (Berber et al., 2016; Chalazonitis et

255   al., 2011). The effects of Hipk misexpression in dopaminergic neurons is of significant interest

256   since these neurons are affected by human neurodegenerative disorders such as Parkinson's

257   disease. Such effects are consistent with the previously mentioned role of mammalian Hipk2 in

258   survival of midbrain dopaminergic neurons (Zhang et al., 2007a).

259   **Effects of Hipk on muscle**

260   Our results demonstrate that Hipk is present in muscle nuclei where Hipk likely phosphorylates

261   transcription factors and other substrates. Interestingly, we have also found that muscle-specific

262   knockdown in *Drosophila* adults dramatically shortens their lifespan and that death is preceded

263   by progressive immobility supporting our claim that muscle and neuronal function are regulated

264   by Hipk. Under control conditions Hipk is predominantly intranuclear where it is found in small

265   puncta, as described previously (Huang et al., 2011). As previous work did not clearly localize

266   these puncta to identified subnuclear structures they have been referred to as 'Hipk domains'

267   (Moller et al., 2003). In some cases, Hipk localization has been associated with the subnuclear

268   promyelocytic leukemia (PML) body where Hipk2-mediated phosphorylation of p53 occurs

269   (Moller et al., 2003). The exact nature of the Hipk nuclear domains is still unresolved, and the

270   appearance of the nuclear structures differs between endogenous proteins and following ectopic

271   expression of Hipk. In *Drosophila*, nuclear localization of Hipk is dependent on the small

272   ubiquitin-related modifier (SUMO) protein (Smt3) and the sumoylation-controlled balance

273   between nuclear and cytoplasmic Hipk has been shown to regulate the JNK signaling pathway

274   (Huang et al., 2011). We found that overexpression of Hipk in muscle results in very large

275   nuclear Hipk-domains having a 'rim' of strong Hipk immunoreactivity with less labelling in the

276   core of these structures. As these structures were much larger than the Hipk domains in wild-

277   type, it is possible that they comprise regions of aggregated Hipk. The structures were confined

278   to the nucleus, with no evidence of large cytoplasmic Hipk-positive structures. Within the

279   nucleus the Hipk domains were extra-nucleolar and were exclusively present in the

280   extrachromosomal regions of the nucleus.

281   **Effects of Hipk on NMJ**

282   To evaluate the possible mechanism of Hipk action at the NMJ and muscle we studied NMJs in

283   Hipk over-expressing animals and found that terminal axonal branching onto these muscles was

284   significantly larger than controls. We found that these NMJ boutons had a striking reduction in

285   levels of phosphorylated Hts, which could be related to the axonal branching effect. Adducin/Hts

286   is an actin- and Spectrin- binding protein that is present both pre- and post-synaptically in the fly

287   NMJ. It is regulated by phosphorylation and we have found that phosphorylated Adducin (p-

288   Add) modulates levels of transcripts of the important protein kinases CaMKII and PAR-1 (Wang

289   et al., 2011, 2014). Thus, our observations that Hipk is associated with reductions in p-Add at the

290   synapse as well as decreased transcripts and immunoreactivity of CaMKII and PAR-1 in the

291   synapse might be of functional significance and a consequence of Hipk action. We would predict

292   that the reductions in phosphorylation of Adducin with Hipk overexpression cause Add to

293   remain at the synapse and lead to the increase in NMJ surface area observed in the Hipk over-

294   expressors.

295   To further extend observations on the Hipk nuclear functions we examined several proteins that

296   are well known to be expressed in fly muscle nuclei including Caz and TBPH/TDP-43. These

297   proteins have been studied extensively, as TDP-43 redistribution from the nucleus to the

11

298   cytoplasm is frequently observed both in the neurodegenerative disorder, amyotrophic lateral

299   sclerosis (ALS) and in fly models of ALS (Casci and Pandey, 2015; Chang and Morton, 2017).

300   In wild-type tissue, TBPH is enriched in nuclear structures or aggregates, some of which overlap

301   with endogenous Hipk proteins. We evaluated TBPH localization in individual Hipk over-

302   expressing larval muscle nuclei. Under these conditions, we observed a striking decrease in

303   nuclear TBPH immunoreactivity and de-localization of TBPH such that the nuclear and

304   cytoplasmic levels were similarly low. These findings suggest that Hipk may regulate TBPH

305   distribution either directly or indirectly. In contrast, another nuclear protein involved in

306   neurodegeneration, Caz, is not clearly affected by Hipk modulation suggesting that the effects

307   we observe with TBPH are not simply generic effects on nuclear proteins.

308   Our results are also of interest in relation to recent work showing that activation of Hipk2

309   promotes endoplasmic reticulum (ER) stress and neurodegeneration in an animal model of ALS

310   (Lee et al., 2016). The effect of Hipk2 in ALS may be mediated by TDP-43, as well as the JNK

311   signaling pathway. Cytosolic TDP-43 is often found to be phosphorylated in tissue from ALS

312   patients and an elevation of phosphorylated Hipk2 (at S359/T360) was found to be positively

313   correlated with the level of ubiquitinated TDP-43 in tissue from ALS patients, post-mortem (Lee

314   et al., 2016). Hipk2 inhibition reduced the neurodegeneration associated with ER stress *in vitro*

315   produced either by tunicamycin or by altered expression of wt or mutant TDP-43 (Lee et al.,

316   2016). Interestingly, mice having mutations in FUS/TLS that are associated with familial ALS

317   did not demonstrate the altered Hipk2 levels, consistent with our observations that Hipk over-

318   expression did not alter the distribution of nuclear Caz [*Drosophila* FUS], or produce a rough

319   eye phenotype with Caz over-expression. However, it is possible that given the many signaling

320   pathways that are triggered by Hipk, other potential mechanisms for neurotoxicity exist. For

321   instance, Hipk2 has also been linked to transcriptional control of N-methyl-D-aspartate

322   receptors, which are well established to be involved in neuronal cell death (Shang et al., 2018).

323   Our data demonstrate that in addition to having roles in tumorigenesis Hipk also has profound

324   effects on the nervous system and muscle including on the NMJ. This work also indicates that in

325   addition to modifying phosphorylation of nuclear proteins, Hipk affects the distribution of

326   nuclear proteins and also can influence the phosphorylation state of extra-nuclear proteins, either

327   directly or indirectly affecting function and viability.

12

328

329

Materials and Methods

331

Fly Stocks

All stocks were maintained at 25°C or 18°C. The *UAS-hipk*-RNAi (NIG) line (17090R-1) used

for most of the current work was obtained from the NIG stock centre. A second *UAS-hipk*-RNAi

(V2) line (108254) used for some crosses was obtained from the VDRC stock centre. *UAS-HA-*

hipk is described in (Lee et al., 2009a) and attP40 *UAS-HA-hipk* in Tettweiler et al., 2019 (in

preparation). The following lines were obtained from the Bloomington *Drosophila* Stock Center:

w^{1118} (3605); w^{1118}; P{UAS-Dcr-2.D}2 (Dicer-2 on chromosome 2; 24650); w^*; P{tubP-

Gal80^{ts}}20; TM2/TM6B, Tb (Gal80^{ts} on chromosome 3; 7019 P{tubP-Gal80^{ts}}2 (Gal80^{ts} on

chromosome 3; 7017); *y w*; *P{Gal4-Mef2.R}3 (Mef2-Gal4*; 27390); *ple-Gal4* (8848); *ChAT-*

Gal4.7.4-19B (6798); *ChAT-DD. Gal4.VP16* (64410); *GawB elav*^{C155} *(elav-Gal4*; 458); *GawB V*

Glut^{OK371} (26160); *GawB D42* (8816); *repo-Gal4* (7415); w^*; *P{longGMR-Gal4}2* (*longGMR-*

Gal4; *8605*); *y w*; *wg*$^{Sp-1}$/*CyO*; *P{longGMR-Gal4}3/TM2* (*longGMR-Gal4*; 8121). The *Appl-*

Gal4 line was kindly provided by Dr. U. Pandey. The *UAS-TBPH* and *UAS-caz* lines were kindly

provided by Dr. B. McCabe. The *TH-Gal4* line was kindly provided by Dr. D. Allan. The

following stocks were constructed for the adult survival experiments and analysis of eye effects:

(i) *UAS-hipk-RNAi/UAS-hipk-RNAi; Gal80^{ts}/Gal80^{ts}* (ii) *Gal80^{ts}/Gal80^{ts}; UAS-HA-hipk/UAS-*

HA-hipk (iii) *Gal80^{ts}/Gal80^{ts}; Tub-Gal4/TM3, Sb* (iv) *Dicer-2/Dicer-2; Tub-Gal4/TM3, Sb Ser*;

(v) attP40 *UAS-HA-hipk/CyO; longGMR-Gal4/longGMR-Gal4*.

Fly crosses, lifespan and phenotypic analyses

Two different sets of crosses were used for lifespan analysis. In the first set, homozygous UAS-

hipk-RNAi (NIG) or *UAS-HA-hipk* females were crossed to *Gal80^{ts}/Gal80^{ts}; Tub-Gal4/TM3, Sb*

males. In the second set, doubly homozygous *UAS-hipk-RNAi* (NIG); *Gal80ts* males were

crossed separately to *Dicer-2/Dicer-2; Tub-Gal4/TM3, Sb* females or homozygous *Mef2-Gal4* or

TH-Gal4 females. These crosses were set up at 18°C and the parents were sub-cultured twice or

three times to fresh medium at three-day intervals and the progeny were allowed to develop to

eclosion at 18°C. Relevant experimental and internal control males from these crosses (see the

13

358   Results), as well as Oregon-R (+) control males raised under the same conditions, were collected

359   within 0-24 hours post-eclosion and shifted to 29°C (10 flies/vial). Thereafter, the males were

360   transferred to fresh medium, usually every 2 or 3 days, and the number of survivors was recorded

361   at each transfer, in most cases until the last of the flies had died. The data were converted to

362   percent survival and these values were plotted versus days at 29°C. For the first set of crosses,

363   there were two trials each for knockdown, over-expression and two types of internal controls and

364   three trials for Oregon-R controls. Lethal phase (LP) refers to the particular stage of development

365   (e.g. larvae, pupae) when death usually occurred.

366

367   Crosses were conducted to test for possible developmental effects of Hipk knockdown or Hipk

368   over-expression in the nervous system and muscles at 29°C in two separate sets of experiments.

369   In the first, most crosses involved mating *Gal4*-driver-bearing males to heterozygous females

370   bearing either NIG *UAS-hipk-RNAi* or *UAS-hipk* transgenes and appropriate balancer

371   chromosomes (*CyO* or *TM3, Sb* or *TM3, Sb Ser*); the single exception involved the glial cell

372   crosses, which used repo-*Gal4*/*TM3, Sb* females and *hipk*-transgene-bearing males. In the

373   second set of experiments, most crosses involved mating females bearing either V2 *UAS-hipk*-

374   RNAi/CyO or attP40 *UAS-hipk*/CyO to *Gal4*-driver-bearing males; the single exception

375   involved tests with the *Appl-Gal4* driver, for which reciprocal crosses were performed. In all

376   cases, crosses were carried out in vials with ~four pairs of parents per vial and the crosses were

377   sub-cultured on fresh medium twice at 3-day intervals. Wherever crosses showed lethality,

378   approximate lethal phases were determined, and any phenotypes of survivors were also noted. In

379   addition, with respect to the first set of experiments, the eyes of surviving *elav-Gal4*/+; *UAS-*

380   *hipk-RNAi*/+, *elav-Gal4*/+; *UAS-hipk*/+ females, as well as those of respective internal control

381   *elav-Gal4*/+; *CyO*/+ and *elav-Gal4*/+; *TM3, Sb*/+ flies, were photographed.

382

383   To test for eye-specific effects of Hipk knockdown and over-expression, NIG *UAS-hipk-*

384   RNAi/*CyO* and 3M *UAS-hipk*/*TM3, Sb* females were crossed separately to *longGMR-Gal4*

385   (chromosome 2) males at 29°C (four pairs of parents per vial) and the crosses were sub-cultured

386   on fresh medium twice at three-day intervals. *UAS-hipk-RNAi*/*longGMR-Gal4* flies failed to

387   eclose at 29°C (data not shown; see Results). After eclosion, the eyes of *longGMR-Gal4*/+; *UAS-*

388   *hipk*/+ females and of internal control *CyO*/*longGMR-Gal4* and *longGMR-Gal4*/+; *TM3, Sb*/+

14

389   females, were photographed. Since pilot studies revealed that attP40 *UAS-hipk*/*longGMR-Gal4*

390   *f*lies developing at 29°C did not exhibit an eye phenotype (data not shown), we used this line to

391   test for potential interactions involving simultaneous Hipk over-expression and over-expression

392   of nuclear proteins of interest, Caz and TBPH. For this analysis, attP40 *UAS-HA-hipk*/*CyO*;

393   *longGMR-Gal4*/*longGMR-Gal4* females were mated separately to homozygous *UAS-caz* and

394   *UAS-TBPH* males at 29°C (four pairs of parents per vial) and the crosses were sub-cultured on

395   fresh medium twice at three-day intervals. In all cases, after eclosion the eyes of appropriate

396   experimental and internal control flies were photographed (see Results for genotypes). In

397   addition, the eyes of surviving *elav-Gal4*/+; *UAS-hipk-RNAi*/+ and *elav-Gal4*/+; *UAS-hipk*/+ and

398   appropriate internal control females from the aforementioned developmental crosses, were also

399   photographed.

400

401   *Larval Body Wall Preparation*

402   Body wall dissections of crawling third instar larvae were performed as previously described

403   (Wang et al., 2015). For transgenic analysis, homozygous *UAS*-transgene-bearing males were

404   crossed to homozygous *Gal4*-bearing virgin females ensuring that all progeny carried one copy

405   of each. All crosses were maintained at 25°C unless indicated otherwise.

406

407   *Immunohistochemistry (IHC)*

408   Immunostaining of body walls was performed as previously described (Ramachandran and

409   Budnik, 2010). The following primary antibodies were used: 1:100 goat anti-Hrp (Jackson

410   ImmunoResearch – 123-005-021); 1:100 rabbit anti-Hrp (JIR – 323-065-021); 1:200 rabbit anti-

411   Hipk (Blaquiere et al., 2018); 1:50 mouse anti-GluRIIA (Developmental Studies Hybridoma

412   Bank – 8B4D2); 1:10 mouse anti-α-Spec (DSHB – 3A9); 1:2 mouse anti-Fas2 (DSHB – 1D4);

413   1:10 mouse anti-Hts (DSHB – 1B1); 1:100 goat anti-phospho-Add^{S662} (Santa Cruz

414   Biotechnology – sc-12614); 1:200 mouse anti-CaMKII (Cosmo Bio – CAC-TNL-001-CAM);

415   1:200 rabbit anti-PAR-1(Sun et al., 2001), which was generously provided by Dr. Bingwei Lu

416   (Stanford University); 1:200 rabbit anti-phospho-Dlg^{S797} (Zhang et al., 2007b), also from Dr. Lu;

417   1:200 rabbit anti-Caz (Sasayama et al., 2012), kindly given by Dr. Takahiko Tokuda (Kyoto

418   Prefectural University); and 1:200 guinea pig anti-TBPH (Swain et al., 2016), a gift from Dr.

419   Dale Dorsett (Saint Louis University). Fluorescent-labeled secondary antibodies from JIR and

15

420   Vector Laboratories were all used at a 1:200 dilution. Stained body walls were mounted in

421   VECTASHIELD Mounting Medium with DAPI (Vector – H-1200). Experiments and their

422   controls were immunostained in the same tube, and thus exposed to the same treatment. Images

423   of NMJs innervating muscles 6/7 from abdominal segment 3 were taken as merged stacks, unless

424   otherwise stated, on either a Nikon A1R laser scanning confocal microscope with NIS-Elements

425   software or a Zeiss LSM 880 with Airyscan, with experiments and their controls imaged under

426   identical acquisition settings. All images were processed with Adobe Photoshop.

427

428   *Fluorescent in situ Hybridization (FISH)*

429   FISH of body walls was performed as previously described (Wang et al., 2014). cDNA clones

430   (*Drosophila* Genomics Resource Center) IP15240 and RE47050 were used as templates to make

431   DIG-labeled, antisense probes against *camkII* and *par-1* transcripts, respectively. Both cDNA

432   clones were obtained from the *Drosophila* Genomics Resource Center. Experiments and their

433   controls were processed in the same tube, and thus exposed to the same treatment. Body walls

434   were mounted and imaged as described in the previous section.

435

436   *Quantifications*

437   Stacked confocal images of larval muscles 6/7 from abdominal segment 3 were used for

438   measurements. Student's t-test was used for statistical analysis, and data was expressed as the

439   mean ± S.E.M. <u>NMJ size</u>: For each NMJ, Hrp immunofluorescence signal was delineated using

440   Photoshop tools and the size was measured as pixel surface area. The outline of muscles 6/7 was

441   also selected with Photoshop and the pixel surface area was recorded. To normalize the NMJ size

442   measurement, the NMJ pixel surface area was divided by the muscle pixel surface area.

443   <u>Immunofluorescence intensity at the NMJ</u>: Quantification of post-synaptic protein levels at the

444   NMJ was calculated as a ratio between the fluorescence intensity of the protein of interest and

445   Hrp, which was used as a control. Immunofluorescence signal at the NMJ was selected using

446   Photoshop, and the intensity was determined by measuring the mean gray value. <u>Puncta levels in</u>

447   <u>the muscle</u>: For quantification of *camkII*/*par-1* FISH puncta or p-Dlg IHC puncta in the muscle,

448   confocal images were inverted and the threshold function of ImageJ was used to create binary

449   images in which puncta were represented by black pixels and the background was eliminated.

16

450   The number of extra-synaptic black pixels within a fixed area size was measured in both muscles

451   6 and 7.

452

462

463

464   **References**

465   Aikawa, Y., Nguyen, L.A., Isono, K., Takakura, N., Tagata, Y., Schmitz, M.L., Koseki, H., and

466   Kitabayashi, I. (2006). Roles of HIPK1 and HIPK2 in AML1- and p300-dependent transcription,

467   hematopoiesis and blood vessel formation. EMBO J *25*, 3955–3965.

468   Berber, S., Wood, M., Llamosas, E., Thaivalappil, P., Lee, K., Liao, B.M., Chew, Y.L., Rhodes,

469   A., Yucel, D., Crossley, M., et al. (2016). Homeodomain-Interacting Protein Kinase (HPK-1)

470   regulates stress responses and ageing in C. elegans. Sci. Rep. *6*, 19582.

471   Blaquiere, J.A., and Verheyen, E.M. (2017). Homeodomain-Interacting Protein Kinases: Diverse

472   and Complex Roles in Development and Disease. Curr. Top. Dev. Biol. *123*, 73–103.

473   Blaquiere, J.A., Lee, W., and Verheyen, E.M. (2014). Hipk promotes photoreceptor

474   differentiation through the repression of Twin of eyeless and Eyeless expression. Dev Biol *390*,

475   14–25.

476   Blaquiere, J.A., Wong, K.K.L., Kinsey, S.D., Wu, J., and Verheyen, E.M. (2018).

17

Homeodomain-interacting protein kinase promotes tumorigenesis and metastatic cell behavior. Dis. Model. Mech. *11*, dmm031146.

Buratti, E., and Baralle, F.E. (2001). Characterization and Functional Implications of the RNA Binding Properties of Nuclear Factor TDP-43, a Novel Splicing Regulator of *CFTR* Exon 9. J. Biol. Chem. *276*, 36337–36343.

Casci, I., and Pandey, U.B. (2015). A fruitful endeavor: Modeling ALS in the fruit fly. Brain Res. *1607*, 47–74.

Chalazonitis, A., Tang, A. a, Shang, Y., Pham, T.D., Hsieh, I., Setlik, W., Gershon, M.D., and Huang, E.J. (2011). Homeodomain interacting protein kinase 2 regulates postnatal development of enteric dopaminergic neurons and glia via BMP signaling. J. Neurosci. *31*, 13746–13757.

Chang, J.-C., and Morton, D.B. (2017). Drosophila lines with mutant and wild type human TDP-43 replacing the endogenous gene reveals phosphorylation and ubiquitination in mutant lines in the absence of viability or lifespan defects. PLoS One *12*, e0180828.

Chen, J., and Verheyen, E.M. (2012). Homeodomain-Interacting Protein Kinase Regulates Yorkie Activity to Promote Tissue Growth. Curr. Biol. *22*, 1582–1586.

Chou, C.-C., Zhang, Y., Umoh, M.E., Vaughan, S.W., Lorenzini, I., Liu, F., Sayegh, M., Donlin-Asp, P.G., Chen, Y.H., Duong, D.M., et al. (2018). TDP-43 pathology disrupts nuclear pore complexes and nucleocytoplasmic transport in ALS/FTD. Nat. Neurosci. *21*, 228–239.

Doxakis, E., Huang, E.J., and Davies, A.M. (2004). Homeodomain-interacting protein kinase-2 regulates apoptosis in developing sensory and sympathetic neurons. Curr Biol *14*, 1761–1765.

Han, B., Zhou, R., Xia, C., and Zhuang, X. (2017). Structural organization of the actin-spectrin-based membrane skeleton in dendrites and soma of neurons. Proc. Natl. Acad. Sci. U. S. A. *114*, E6678–E6685.

Huang, H., Du, G., Chen, H., Liang, X., Li, C., Zhu, N., Xue, L., Ma, J., and Jiao, R. (2011). Drosophila Smt3 negatively regulates JNK signaling through sequestering Hipk in the nucleus. Development *138*, 2477–2485.

Inoue, T., Kagawa, T., Inoue-Mochita, M., Isono, K., Ohtsu, N., Nobuhisa, I., Fukushima, M.,

18

504   Tanihara, H., and Taga, T. (2010). Involvement of the Hipk family in regulation of eyeball size,

505   lens formation and retinal morphogenesis. FEBS Lett. *584*, 3233–3238.

506   Isono, K., Nemoto, K., Li, Y., Takada, Y., Suzuki, R., Katsuki, M., Nakagawara, A., and Koseki,

507   H. (2006). Overlapping roles for homeodomain-interacting protein kinases hipk1 and hipk2 in

508   the mediation of cell growth in response to morphogenetic and genotoxic signals. Mol Cell Biol

509   *26*, 2758–2771.

510   Kim, Y.H., Choi, C.Y., Lee, S.J., Conti, M.A., and Kim, Y. (1998). Homeodomain-interacting

511   protein kinases, a novel family of co-repressors for homeodomain transcription factors. J. Biol.

512   Chem. *273*, 25875–25879.

513   Koh, Y.H., Popova, E., Thomas, U., Griffith, L.C., and Budnik, V. (1999). Regulation of DLG

514   localization at synapses by CaMKII-dependent phosphorylation. Cell *98*, 353–363.

515   Krieger, C., Wang, S., Yoo, S.H., and Harden, N. (2016). Adducin at the Neuromuscular

516   Junction in Amyotrophic Lateral Sclerosis: Hanging on for Dear Life. Front. Cell. Neurosci. *10*,

517   doi: 10.3389.

518   Lanson, N.A., Maltare, A., King, H., Smith, R., Kim, J.H., Taylor, J.P., Lloyd, T.E., and Pandey,

519   U.B. (2011). A Drosophila model of FUS-related neurodegeneration reveals genetic interaction

520   between FUS and TDP-43. Hum. Mol. Genet. *20*, 2510–2523.

521   Lee, S., Shang, Y., Redmond, S.A., Urisman, A., Tang, A.A., Li, K.H., Burlingame, A.L., Pak,

522   R.A., Jovičić, A., Gitler, A.D., et al. (2016). Activation of HIPK2 Promotes ER Stress-Mediated

523   Neurodegeneration in Amyotrophic Lateral Sclerosis. Neuron *91*, 41–55.

524   Lee, W., Andrews, B.C., Faust, M., Walldorf, U., and Verheyen, E.M. (2009a). Hipk is an

525   essential protein that promotes Notch signal transduction in the Drosophila eye by inhbition of

526   the global co-repressor Groucho. Dev Biol *325*, 263–272.

527   Lee, W., Andrews, B.C., Faust, M., Walldorf, U., and Verheyen, E.M. (2009b). Hipk is an

528   essential protein that promotes Notch signal transduction in the Drosophila eye by inhbition of

529   the global co-repressor Groucho. Dev Biol *325*, 263–272.

530   Lee, W., Swarup, S., Chen, J., Ishitani, T., and Verheyen, E.M. (2009c). Homeodomain-

531   interacting protein kinases (Hipks) promote Wnt/Wg signaling through stabilization of beta-

19

532   catenin/Arm and stimulation of target gene expression. Development *136*, 241–251.

533   Matsuoka, Y., Li, X., and Bennett, V. (1998). Adducin Is an In Vivo Substrate for Protein Kinase

534   C: Phosphorylation in the MARCKS-related Domain Inhibits Activity in Promoting Spectrin–

535   Actin Complexes and Occurs in Many Cells, Including Dendritic Spines of Neurons. J. Cell Biol.

536   *142*, 485–497.

537   Moller, A., Sirma, H., Hofmann, T.G., Rueffer, S., Klimczak, E., Droge, W., Will, H., and

538   Schmitz, M.L. (2003). PML is required for homeodomain-interacting protein kinase 2 (HIPK2)-

539   mediated p53 phosphorylation and cell cycle arrest but is dispensable for the formation of HIPK

540   domains. Cancer Res *63*, 4310–4314.

541   Pielage, J., Bulat, V., Zuchero, J.B., Fetter, R.D., and Davis, G.W. (2011). Hts/Adducin controls

542   synaptic elaboration and elimination. Neuron *69*, 1114–1131.

543   Poon, C.L.C., Zhang, X., Lin, J.I., Manning, S.A., and Harvey, K.F. (2012). Homeodomain-

544   interacting protein kinase regulates Hippo pathway-dependent tissue growth. Curr. Biol. *22*,

545   1587–1594.

546   Ramachandran, P., and Budnik, V. (2010). Immunocytochemical Staining of *Drosophila* Larval

547   Body-Wall Muscles. Cold Spring Harb. Protoc. *2010*, pdb.prot5470.

548   Rinaldo, C., Siepi, F., Prodosmo, A., and Soddu, S. (2008). HIPKs: Jack of all trades in basic

549   nuclear activities. Biochim. Biophys. Acta - Mol. Cell Res. *1783*, 2124–2129.

550   Sasayama, H., Shimamura, M., Tokuda, T., Azuma, Y., Yoshida, T., Mizuno, T., Nakagawa, M.,

551   Fujikake, N., Nagai, Y., and Yamaguchi, M. (2012). Knockdown of the Drosophila fused in

552   sarcoma (FUS) homologue causes deficient locomotive behavior and shortening of motoneuron

553   terminal branches. PLoS One *7*, e39483.

554   Shang, Y., Zhang, J., and Huang, E.J. (2018). HIPK2-Mediated Transcriptional Control of

555   NMDA Receptor Subunit Expression Regulates Neuronal Survival and Cell Death. J. Neurosci.

556   *38*, 4006–4019.

557   Sun, T.Q., Lu, B., Feng, J.J., Reinhard, C., Jan, Y.N., Fantl, W.J., and Williams, L.T. (2001).

558   PAR-1 is a Dishevelled-associated kinase and a positive regulator of Wnt signalling. Nat Cell

559   Biol *3*, 628–636.

20

560 Swain, A., Misulovin, Z., Pherson, M., Gause, M., Mihindukulasuriya, K., Rickels, R.A.,

561 Shilatifard, A., and Dorsett, D. (2016). Drosophila TDP-43 RNA-Binding Protein Facilitates

562 Association of Sister Chromatid Cohesion Proteins with Genes, Enhancers and Polycomb

563 Response Elements. PLoS Genet. *12*, e1006331.

564 Swarup, S., and Verheyen, E.M.E.M. (2011). Drosophila homeodomain-interacting protein

565 kinase inhibits the Skp1-Cul1-F-box E3 ligase complex to dually promote Wingless and

566 Hedgehog signaling. Proc Natl Acad Sci U S A *108*, 9887–9892.

567 Thurmond, J., Goodman, J.L., Strelets, V.B., Attrill, H., Gramates, L.S., Marygold, S.J.,

568 Matthews, B.B., Millburn, G., Antonazzo, G., Trovisco, V., et al. (2019). FlyBase 2.0: The next

569 generation. Nucleic Acids Res. *47*, D759–D765.

570 Wang, S., Sanny, J., Lee, J., Dong, K., Harden, N., Yang, J., Tsai, A., Kuca, T., and Krieger, C.

571 (2011). Drosophila adducin regulates Dlg phosphorylation and targeting of Dlg to the synapse

572 and epithelial membrane. Dev. Biol. *357*, 392–403.

573 Wang, S., Tsai, A., Wang, M., Yoo, S., Kim, H. -y., Yoo, B., Chui, V., Kisiel, M., Stewart, B.,

574 Parkhouse, W., et al. (2014). Phospho-regulated Drosophila adducin is a determinant of synaptic

575 plasticity in a complex with Dlg and PIP2 at the larval neuromuscular junction. Biol. Open *3*,

576 1196–1206.

577 Wang, S., Yoo, S., Kim, H., Wang, M., Zheng, C., Parkhouse, W., Krieger, C., and Harden, N.

578 (2015). Detection of In Situ Protein-protein Complexes at the Drosophila Larval Neuromuscular

579 Junction Using Proximity Ligation Assay. J. Vis. Exp. *95*, 52139.

580 Wiggins, A.K., Wei, G., Doxakis, E., Wong, C., Tang, A.A., Zang, K., Luo, E.J., Neve, R.L.,

581 Reichardt, L.F., and Huang, E.J. (2004). Interaction of Brn3a and HIPK2 mediates

582 transcriptional repression of sensory neuron survival. J Cell Biol *167*, 257–267.

583 Xu, K., Zhong, G., and Zhuang, X. (2013). Actin, Spectrin, and Associated Proteins Form a

584 Periodic Cytoskeletal Structure in Axons. Science (80-.). *339*, 452–456.

585 Zhang, J., Pho, V., Bonasera, S.J., Holtzman, J., Tang, A.T., Hellmuth, J., Tang, S., Janak, P.H.,

586 Tecott, L.H., and Huang, E.J. (2007a). Essential function of HIPK2 in TGFbeta-dependent

587 survival of midbrain dopamine neurons. Nat Neurosci *10*, 77–86.

588   Zhang, Y., Guo, H., Kwan, H., Wang, J.-W., Kosek, J., and Lu, B. (2007b). PAR-1 Kinase

589   Phosphorylates Dlg and Regulates Its Postsynaptic Targeting at the Drosophila Neuromuscular

590   Junction. Neuron *53*, 201–215.

591

592

Figure Legends

Fig. 1: Ubiquitous modulation of Hipk affects adult life span. Adult males subjected to Hipk knockdown (*UAS-hipk^{RNAi}*: NIG *UAS-hipk-RNAi/Gal80^{ts}*; *Tub-Gal4*/+; light red and dark red curves; n= 89 and n= 65) died within 2 to 4 days at 29°C. Adult males subjected to Hipk over-expression (*UAS-hipk-RNAi*: 3M *UAS-hipk/Gal80^{ts}*; *Tub-Gal4*/+; purple curves; n= 69 and n= 107) died within 7-10 days at 29°C. In contrast, Ore-R control males (n= 110; n= 96 and n= 69; light grey, dark grey and intermediate grey curves) died primarily within 25 to 40 days at 29°C, whereas internal control males (*TM3, Sb*: *UAS-hipk-RNAi/Gal80^{ts}*; *TM3, Sb*/+ or *Gal80^{ts}*/+; *UAS-hipk/TM3, Sb*; blue-purple curves; n= 69, n= 50, n= 109 and n= 60) died primarily within 21 to 25 days at 29°C.

Fig. 2: Disrupted eye patterning due to modulation of Hipk at 29°C. The eyes of internal control females (A: *elav*/+; *CyO*/+; C: *elav*/+; *TM3, Sb*/+; E: *longGMR-Gal4*/+; *TM3, Sb*/+) are normal. In contrast, the eyes of (B) *elav*/+; *UAS-hipk-RNAi*/+ and (D) *elav*/+; *UAS-hipk* (3M)/+ females are rough, whereas those of (F) *longGMR-Gal4*/+; *UAS-hipk*/+ females are smooth and have somewhat reduced pigmentation. No *UAS-hipk-RNAi/longGMR-Gal4* flies survived at 29°C or 25°C (data not shown).

Fig. 3: Hipk is present throughout the muscle cytoplasm and within muscle nuclei during larval NMJ development. (A-A''') In wild-type control (i.e. *Mef2-Gal4* outcrossed to *w^{1118}*) larval body wall muscles, Hipk showed an extra-synaptic punctate distribution throughout the muscle cytoplasm and within muscle nuclei, which were marked with DAPI. No distinct accumulations were observed at the NMJ, which was marked by Hrp. (B-B''') Muscle-specific expression of *UAS-hipk* with *Mef2-Gal4* led to increased Hipk puncta in the muscle cytoplasm. Most strikingly, Hipk also accumulated within muscle nuclei as large, round bodies. (C-D'') Magnified, single-sectional views of muscle nuclei. For the wild-type control, Hipk puncta were found within the nucleus, primarily in DAPI-negative regions (C-C'', see cross-sectional views in the panels directly below). With Hipk over-expression in the muscle, Hipk was present at both the boundary and within the nuclear bodies, which were also localized in DAPI-negative regions (D-D'', see cross-sectional views). (E) Quantification of the effects of Hipk on NMJ size. NMJ size was measured as NMJ pixel surface area normalized against muscle pixel surface area.

23

624   Over-expression of Hipk in the muscle resulted in significantly larger NMJs when compared to

625   the wild-type control. Sample size was six NMJs per genotype. * p>0.05. Scale bars: 40µm (A-

626   B''); 10uM (C-D'').

627

628   **Fig. 4: Hipk disrupts Hts distribution in the muscle and suppresses its phosphorylation at**

629   **the MARCKS domain.** (A-A'') In the wild-type control, Hts localized to the NMJ. In addition,

630   Hts puncta formed a lattice-like network throughout the muscle. (B-B'') With Hipk over-

631   expression in the muscle, Hts still localized to the post-synaptic membrane of the NMJ.

632   However, the organization of the Hts muscle puncta was disrupted. Cloudy accumulations in the

633   muscle were also often observed. (C-C'') p-Add immunoreactivity in the wild-type control was

634   present at the NMJ, and was also observed as puncta that formed the lattice-like network in the

635   muscle. The antibody detects an Add phosphorylation site in the MARCKS domain, which is

636   conserved in Hts. (D-D'') Muscle-specific over-expression of Hipk reduced p-Add

637   immunoreactivity, as lower signal levels were observed at the NMJ, and the lattice-like network

638   in the muscle was missing. In addition, aberrant accumulations were observed in the cytoplasm.

639   (E-J) High-magnification views of Hts and p-Add immunoreactivity in a section of muscle

640   membrane, showing the lattice-like network in wild-type (E and H) and Hipk over-expression

641   phenotypes, *i.e.* disrupted organization (F and I) and aberrant accumulations (G and J). Scale

642   bars: 40µm (A-D''); 10µm (E-J).

643

644   **Fig. 5: Hipk reduces Dlg phosphorylation through negative regulation of CaMKII and**

645   **PAR-1 expression.** (A) In the wild-type control, CaMKII localized specifically at the NMJ, but

646   was also present throughout the muscle cytoplasmic surface (see cross-section of the muscle in

647   the panel directly below). (B) Muscle-specific Hipk over-expression led to reduced CaMKII

648   levels in the muscle, exposing the underlying striated pattern of the sarcomeres (more easily

649   observed in the cross-section). (C) Similar to CaMKII, PAR-1 in the wild-type control was

650   present at the NMJ and muscle cytoplasmic surface (see cross-section). (D) Hipk over-

651   expression also resulted in lower PAR-1 levels in the muscle (more easily observed in the cross-

652   section). (E-E'') In the wild-type control, *camkII* transcripts were found as distinct

653   accumulations within muscle nuclei, with lower levels of puncta found in the muscle cytoplasm.

654   DAPI was used to mark the nuclei. (F-F'') Over-expression of Hipk in the muscle caused a

24

655   marked decrease in overall *camkII* transcript levels. (G-H'') Similar results were observed for

656   *par-1* transcripts. (I) p-Dlg in the wild-type control was observed at the NMJ and as puncta

657   throughout the muscle cytoplasm. The antibody detects Dlg phosphorylation at the PAR-1 target

658   site in the GUK domain. Inset shows p-Dlg immunoreactivity in a section of muscle that was

659   converted to a black-and-white image. (J) Hipk over-expression resulted in reduced p-Dlg puncta

660   levels in the muscle (compare insets). Scale bars: 40μm (A-D); 20μm (E-H''); 40μm (I,J).

661

662   **Fig. 6: Hipk-mediated effects on the ALS-associated proteins, FUS/Caz and TDP-43/TBPH.**

663   (A) In the wild-type control, Caz localized predominately to muscle nuclei. (B) Muscle-specific

664   over-expression of Hipk caused no observable effects on Caz distribution or levels. (C) TBPH

665   was also most prevalent in muscle nuclei in the wild-type control. (D) Hipk over-expression in

666   the muscle resulted in reduced nuclear TBPH levels. (E-I) Genotypes for eye images (all males

667   incubated at 29°C): *UAS-hipk/+; longGMR-Gal4/+* (E), *UAS-caz/CyO; longGMR-Gal4/+* (F),

668   *UAS-hipk/UAS-caz; longGMR-Gal4/+* (G); *CyO/UAS-TBPH; longGMR-Gal4/+* (H), and *UAS-*

669   *hipk/UAS-TBPH; longGMR-Gal4/+* (I). Scale bar: 40μm (A-D).

670   **Fig. S1: Knockdown of Hipk in adult muscles shortens lifespan, but knockdown in adult**

671   **dopaminergic neurons has no effect.** Adult males subjected to muscle specific Hipk

672   knockdown at 29°C (*UAS-hipk-RNAi*; *Mef2-Gal4*: NIG *UAS-hipk-RNAi/+*; *Mef2-Gal4/Gal80*ts;

673   purple curve; n= 110) died within 11-15 days. Adult Oregon R control males (black curve; n=

674   110) under identical conditions died much later. Adult males subjected to dopaminergic

675   knockdown at 29°C (*UAS-hipk-RNAi*; *TH-Gal4*: *UAS-hipk-RNAi/+*; *TH-Gal4/Gal80*ts; yellow

676   curve; n= 109) showed a lifespan that was similar to that of control males (black curve). The

677   shortened lifespans of males subjected to Hipk knockdown (*UAS-hipk-RNAi*: *UAS-hipk-*

678   *RNAi/Dicer-2*; *Tub-Gal4/Gal80*ts; red curve; n= 59) or over-expression (*Dicer-2/Gal80*ts; *UAS-*

679   *hipk+/Tub-Gal4*; green curve; n= 110) at 29°C were comparable to those described above.

680   **Fig. S2: Hipk knock-down in the muscle during larval NMJ development.** (A) A typical 3rd

681   instar larval NMJ, marked by Hrp, innervating muscles 6/7 in abdominal segment 3. (B) Muscle-

682   specific expression of transgenic *hipk-RNAi* resulted in morphological defects in the muscle.

683   Scale bar: 40μm (A,B).

25

684 **Fig. S3: Hipk-mediated effects on different post-synaptic proteins.** Post-synaptic protein

685 levels at the NMJ was calculated as a ratio between the fluorescence intensity of the protein of

686 interest and Hrp, which was used as a staining control. Immunofluorescence signal at the NMJ

687 was selected using Photoshop, and the intensity was determined by measuring the mean gray

688 value. (A) No significant effects on the levels of GluRIIA at the NMJ were observed between

689 muscle-specific Hipk overexpression and the wild-type control. n = 8 (over 4 body walls) for

690 each genotype. (B) However, Hipk over-expression resulted in significantly lower synaptic

691 levels of α-Spec. n = 6 (over 3 body walls) for each genotype. (D) Hipk over-expression also

692 resulted in significantly higher Fas2 synaptic levels. n = 6 (over 3 body walls) for each genotype.

693 *** p < 0.0001.

694 **Fig. S4: Quantification of FISH and IHC puncta levels in the muscle.** Confocal images were

695 converted to binary images, where immunofluorescent puncta were represented as black pixels

696 and the background was represented as white pixels (examples are shown). The number of extra-

697 synaptic black pixels within a fixed area size was measured. (A) Muscle-specific Hipk over-

698 expression led to significantly reduced levels of *camkII* FISH signal when compared to the wild-

699 type control. n = 20 (over 5 body walls) for each genotype. (B) Similar results were observed for

700 *par-1* FISH signal. n = 16 (over 4 body walls) for each genotype. (C) p-Dlg IHC signal in the

701 muscle was also significantly lowered when Hipk was over-expressed in the muscle. n = 16 (over

702 4 body walls) for each genotype. * p = 0.019; ** p = 0.0007; *** p < 0.0001. Scale bars: 40μm
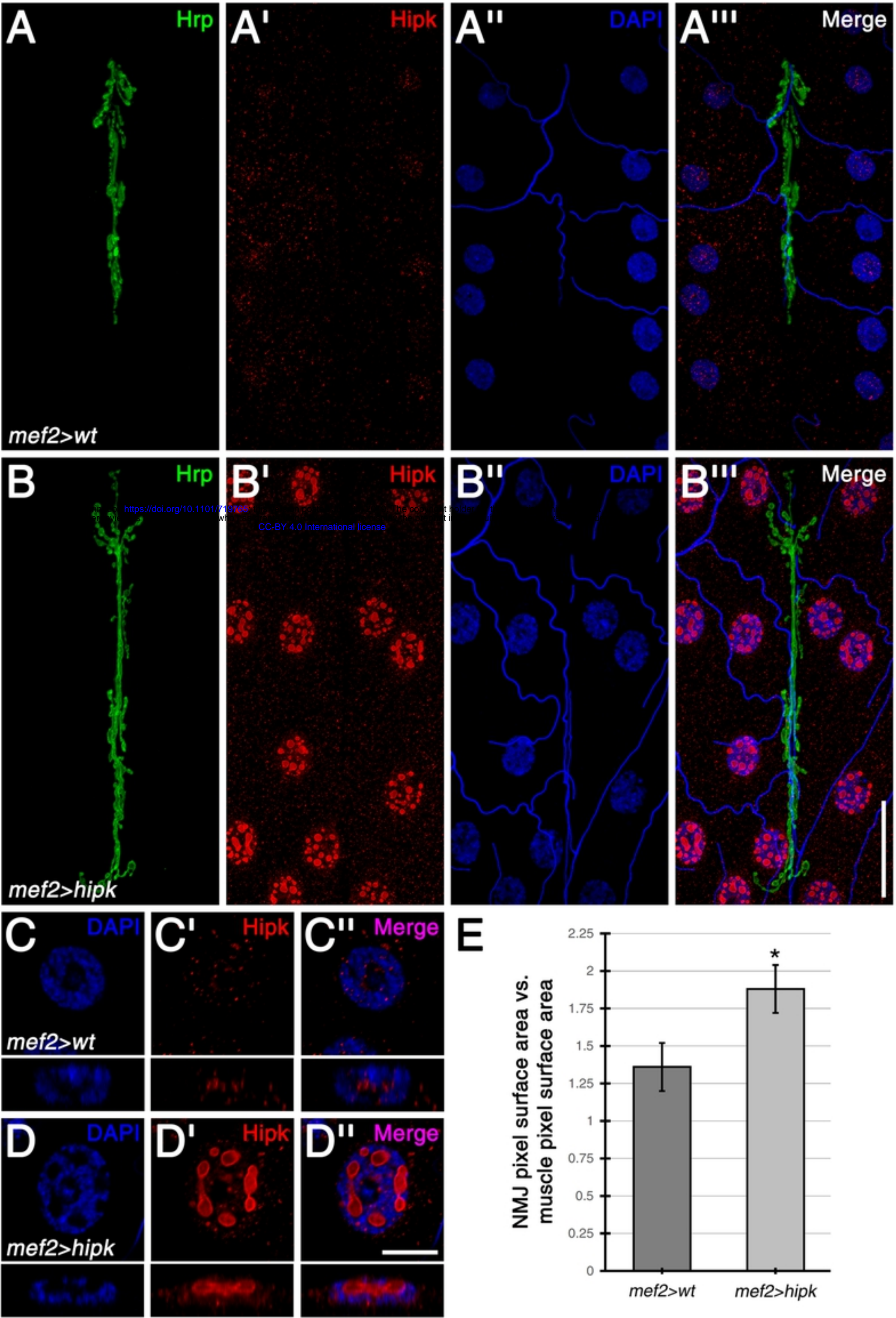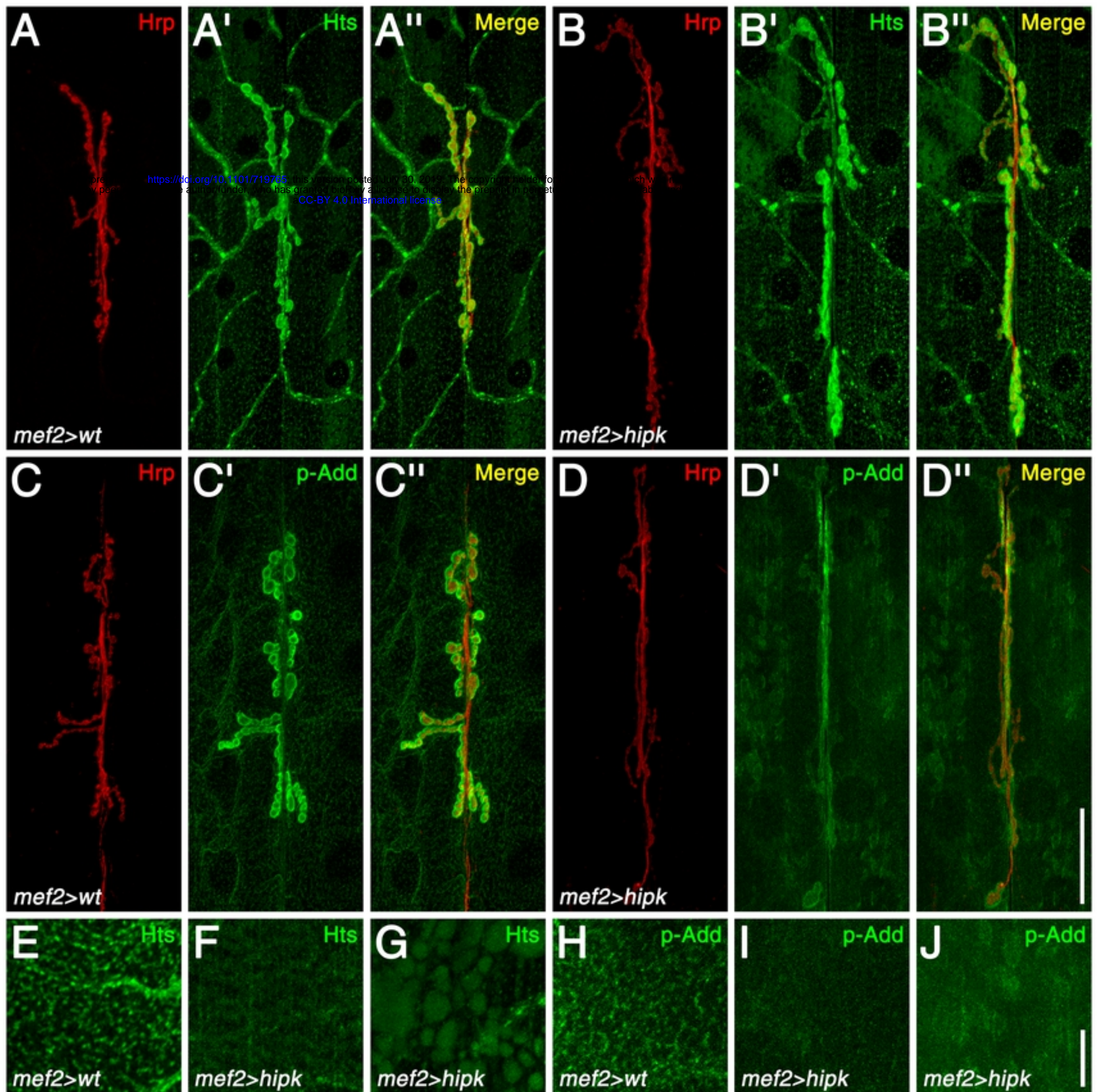
703 (A); 40μm (B); 40μm (C).
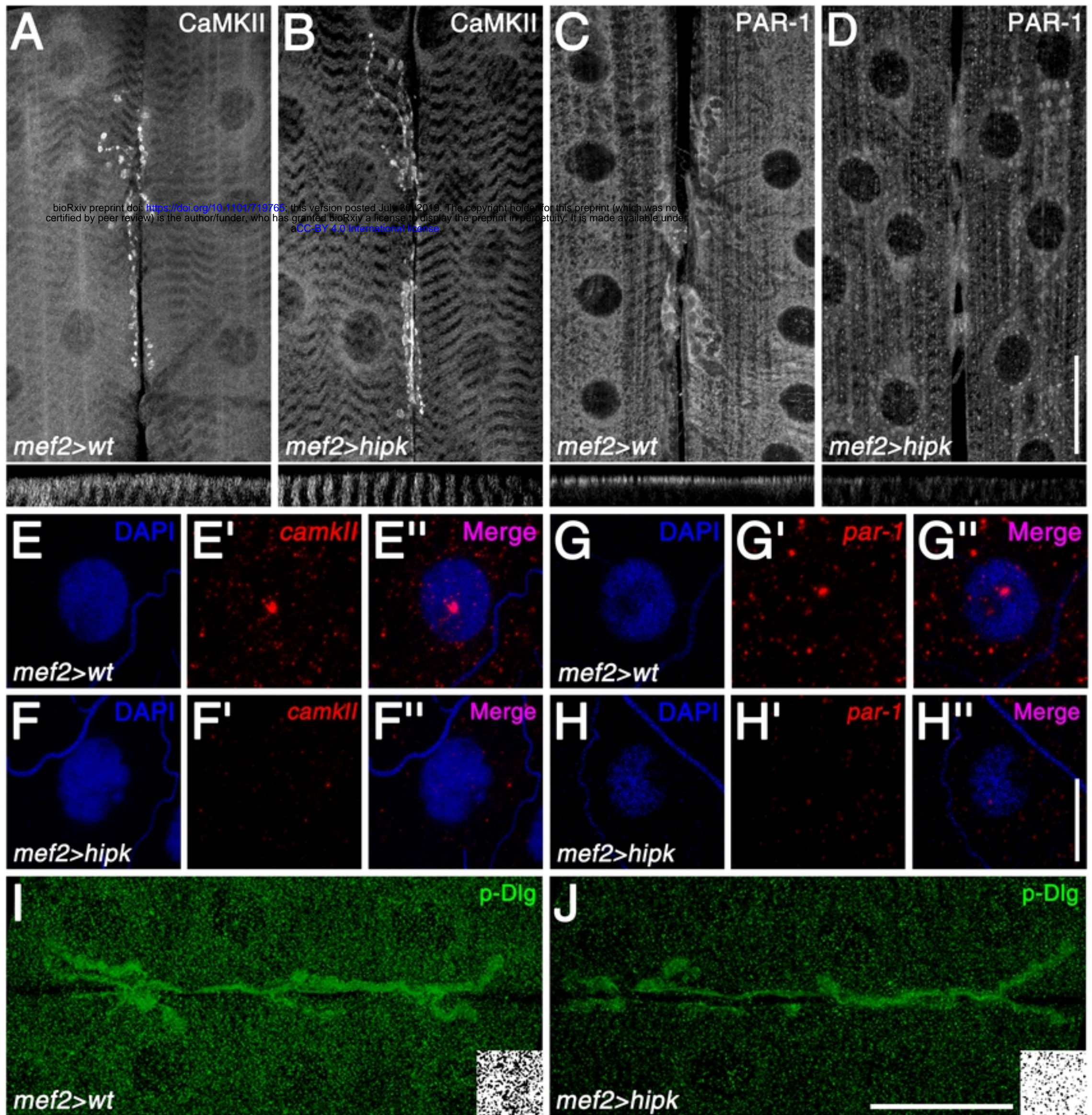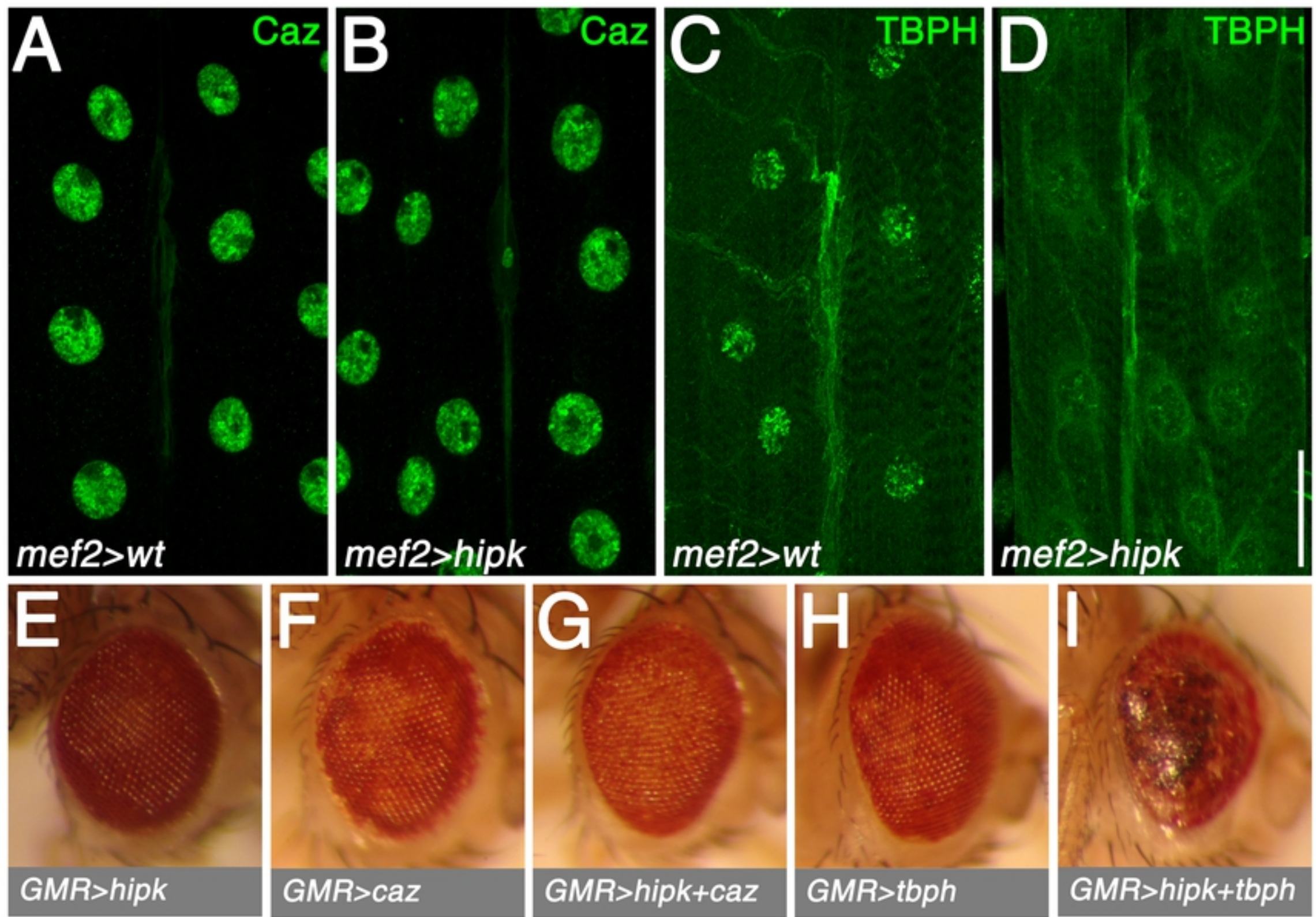
26

Figure 3

Figure 4

Figure 5

Figure 6
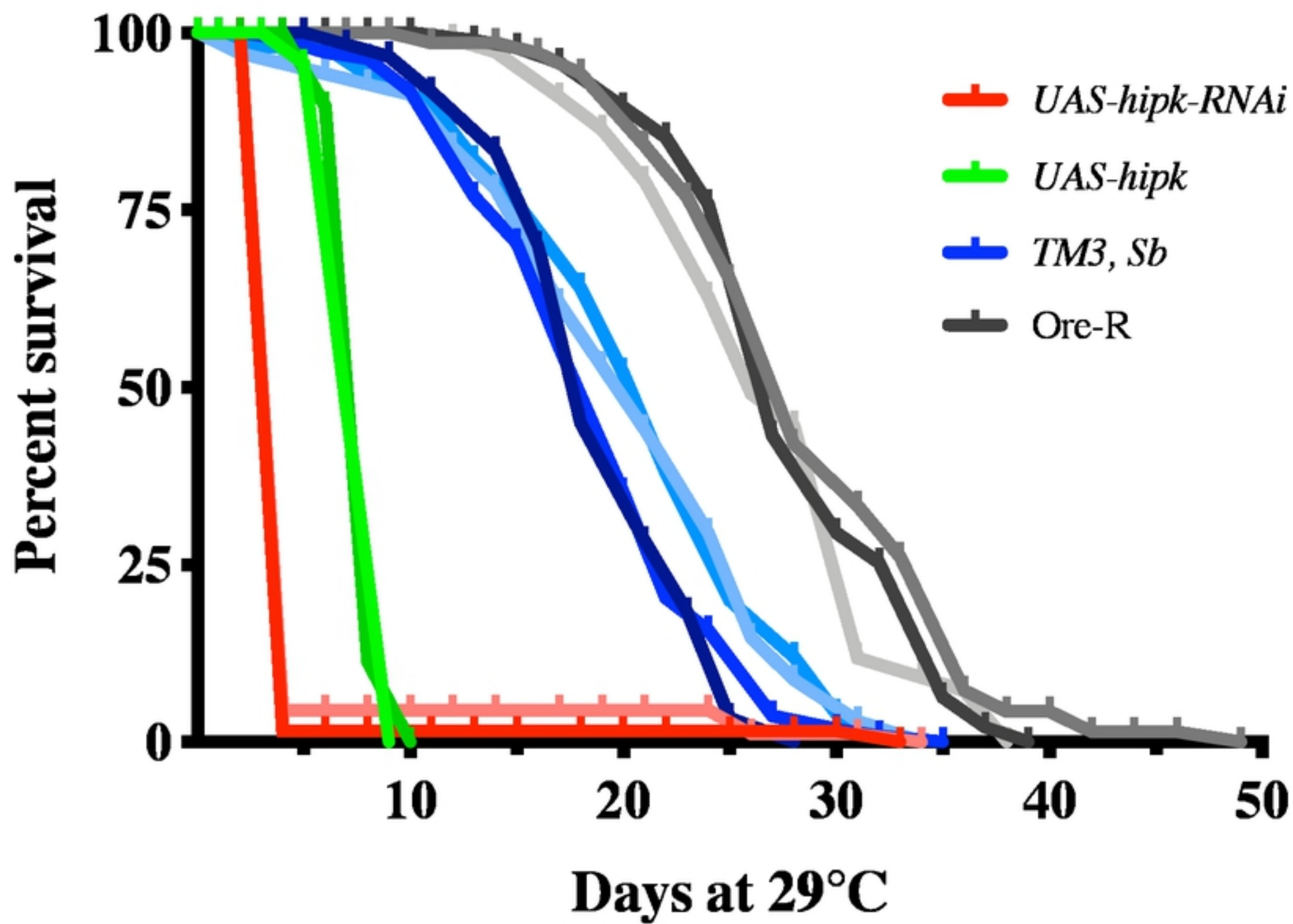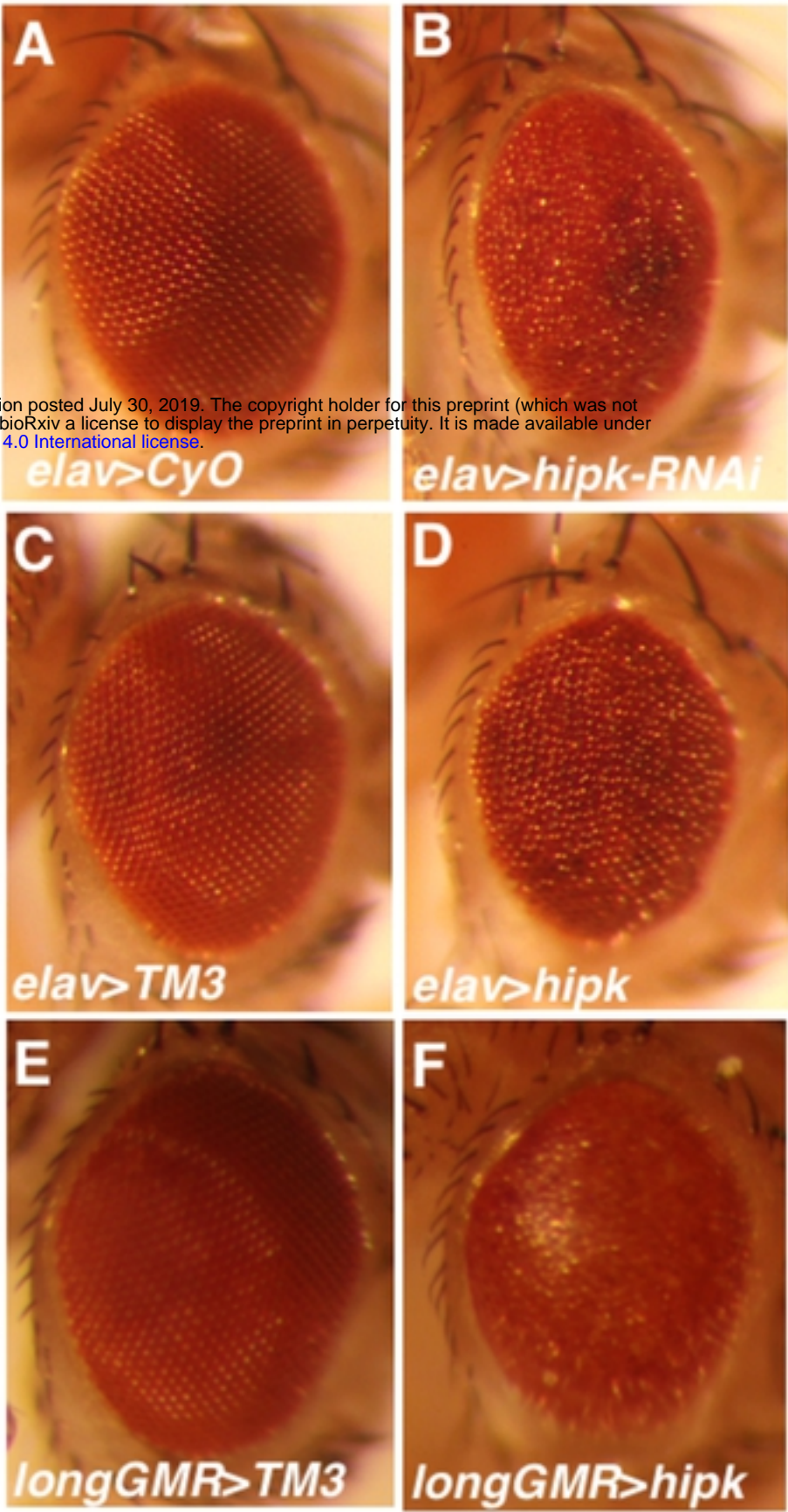
Figure 1

Figure 2

Table 1: Tests for viability of *hipk* knockdown in various nervous system components and muscles using the NIG *UAS-hipk-RNAi*

Gal4 Driver	Expression	% Progeny		Total Flies	Comments on UAS-hipk-RNAi
		UAS-hipk-RNAi	Control (Balancer)		
Appl	Pan-neural	0	100	100	Polyphasic LP, black structures in ventral termini of pupae
GawB elav^C155	Pan-neural	16.4	83.6	165	Pupal LP; variably rough eyes with black patches
ple	Dopaminergic	0	100	255	Larval/pupal LP (undifferentiated)
TH	Dopaminergic	4.3	95.7	115	Larval/pupal LP (undifferentiated)
ChAT-Gal4.19B	Cholinergic	54.2	45.8	96	Viable
ChAT-DD.Gal4.VP16	Cholinergic	51.1	48.9	278	Viable
GawB V Glut^OK371	Glutamatergic	44.1	55.9	177	Viable
GawB D42	Motor-neuron	50.2	49.8	229	Viable
repo	Glial cells	0	100	155	Larval LP
Mef2	Muscle	0	100	157	Pupal LP (undifferentiated)

Table 1

Table 2: Tests for viability of *hipk* over-expression in various nervous system components and muscles using the 3M *UAS-HA-hipk*

| *Gal4* Driver | Expression | % Progeny | | Total Flies | Comments on *UAS-hipk* |
		UAS-HA-hipk	Control (Balancer)		
Appl	Pan-neural	0.9	99.1	106	Larval/pupal LP
GawB elav[C155]	Pan-neural	26.9	73.1	67	Rough eyes
ple	Dopaminergic	0	100	225	Polyphasic LP, some undifferentiated black pupae
TH	Dopaminergic	0	100	158	Larval/pupal LP (undifferentiated)
ChAT-Gal4.7.4.19B	Cholinergic	55.5	44.5	164	Viable
ChAT-DD.Gal4.VP16	Cholinergic	51.1	48.9	278	Viable
GawB V Glut[OK371]	Glutamatergic	54.3	45.7	175	Viable
GawB D42	Motor-neuron	40.1	59.9	142	Viable
repo	Glial cells	0	100	174	Larval LP
Mef2	Muscle	0	100	156	Larval/pupal LP (undifferentiated)

Table 2